Biosensors and Bioelectronics 25 (2010) 1454–1459

Contents lists available at ScienceDirect

Biosensors and Bioelectronics

journal homepage: www.elsevier.com/locate/bios

Development of an implantable D-serine biosensor for *in vivo* monitoring using mammalian D-amino acid oxidase on a poly (*o*-phenylenediamine) and Nafion-modified platinum–iridium disk electrode

Zainiharyati M. Zain[a,b], Robert D. O'Neill[b], John P. Lowry[c], Kenneth W. Pierce[c], Mark Tricklebank[d], Aidiahmad Dewa[e], Sulaiman Ab Ghani[a,*]

[a] *Pusat Pengajian Sains Kimia, Universiti Sains Malaysia, 11800 USM Pulau Pinang, Malaysia*
[b] *UCD School of Chemistry and Chemical Biology, University College Dublin, Belfield, Dublin 4, Ireland*
[c] *Chemistry Department, National University of Ireland, Maynooth, Ireland*
[d] *Eli Lilly and Co. Limited, Windlesham, Surrey, United Kingdom*
[e] *Pusat Pengajian Sains Farmasi, Universiti Sains Malaysia, 11800 USM, Pulau Pinang, Malaysia*

ARTICLE INFO

Article history:
Received 10 September 2009
Received in revised form 29 October 2009
Accepted 29 October 2009
Available online 6 November 2009

Keywords:
Microbiosensor
D-serine
D-amino acid oxidase
Implantable
Neurochemical monitoring

ABSTRACT

D-serine has been implicated as a brain messenger, promoting not only neuronal signalling but also synaptic plasticity. Thus, a sensitive tool for D-serine monitoring in brain is required to understand the mechanisms of D-serine release from glia cells. A biosensor for direct fixed potential amperometric monitoring of D-serine incorporating mammalian D-amino acid oxidase (DAAO) immobilized on a Nafion coated poly-*ortho*-phenylenediamine (PPD) modified Pt–Ir disk electrode was therefore developed. The combined layers of PPD and Nafion enhanced the enzyme activity and biosensor efficiency by ~2-fold compared with each individual layer. A steady state response time ($t_{90\%}$) of 0.7 ± 0.1 s (n = 8) and limit of detection 20 ± 1 nM (n = 8) were obtained. Cylindrical geometry showed lower sensitivity compared to disk geometry (61 ± 7 μA cm^{-2} mM^{-1}, (n = 4), R^2 = 0.999). Interference by ascorbic acid (AA), the main interference species in the central nervous system and other neurochemical electroactive molecules was negligible. Implantation of the electrode and microinjection of D-serine into rat brain striatal extracellular fluid demonstrated that the electrode was capable of detecting D-serine in brain tissue *in vivo*.

1. Introduction

D-serine, a gliotransmitter that modulates neurotransmission at glutamatergic synapses, is found at relatively high concentrations (~6 μM) in the extracellular fluid (ECF) of mammalian forebrain (Hashimoto et al., 1995; Xie et al., 2005). It acts as a co-agonist at the glycine site of the glutamate *N*-methyl-D-aspartate receptor (NMDAr) (Martineau et al., 2006; Matsui et al., 1995; Mothet, 2001) and has been implicated in schizophrenia (Bendikov et al., 2007), cerebral ischemia (Katsuki et al., 2004) and Alzheimer's disease (Nagata et al., 1995). Hence, quantification of D-serine *in vivo* is essential in order to better understand its role in neurophysiological pathways. Chromatography (Berna and Ackermann, 2007; Durkin et al., 1988; Grant et al., 2006; Hashimoto et al., 1992) and electrophoresis (O'Brien, 2005; Quan et al., 2005) are the two conventional techniques used for selective and sensitive enantiomer separation of D-serine in neuroanalysis. Enzyme based amperometric sensors could be a good alternative for enantioselective analysis. In addition, microbiosensors are preferred to microdialysis in monitoring neurochemicals as they provide higher temporal resolution and cause less damage to brain tissue (Duff and O'Neill, 1994; Fumero et al., 1994; Mitala et al., 2008).

The determination of D-serine in rat cortex by incorporating D-amino acid oxidase (DAAO) from recombinant *R. gracillis* has been reported (Pernot et al., 2008). Such a device is based on stereospecific oxidative deamination of neutral D-serine, catalysed by DAAO to the corresponding imino acids (Eq. (1)), which is the rate-limiting step of the overall reactions. The reduced flavin adenine dinucleotide ($FADH_2$) produced is oxidized by oxygen to generate hydrogen peroxide (Eq. (2)) prior to imino acid dissociation from the enzyme active centre producing α-keto-3-hydroxypropanoic acid and ammonium ions through a non-enzymatic reaction (Eq. (3)) (Pilone, 2000).

$$HOCH_2CHNH_2COOH + DAAOFAD \rightarrow HOCH_2C{=}NHCOOH + DAAOFADH_2 \quad (1)$$

$$FADH_2 + O_2 \rightarrow FAD + H_2O_2 \quad (2)$$

$$HOCH_2C{=}NHCOOH + H_2O \rightarrow HOCH_2COCOOH + NH_3 \quad (3)$$

* Corresponding author. Tel.: +6 04 653 4030; fax: +6 04 6574854.
E-mail address: sag@usm.my (S. Ab Ghani).

0956-5663/$ – see front matter © 2009 Elsevier B.V. All rights reserved.
doi:10.1016/j.bios.2009.10.049

It has previously been reported (Killoran and O'Neill, 2008) that poly-*ortho*-phenylenediamine is the best phenylenediamine isomer for use in the design of a permselective layer for micro implantable Pt/Ir based biosensors. This isomer is superior in blocking AA compared to *meta* isomer for AA levels greater than 200 μM. This work evaluates, among other issues, the sensitivity and selectivity of different designs, response time, pH effects, the effective enzyme activity and biosensor efficiency which are also essential in biosensor characterization (O'Neill et al., 2008) mainly for *in vivo* utilization.

2. Experimental

2.1. Chemicals

All chemicals used were of analytical grade purchased from Sigma–Aldrich Chemicals (Schnelldorf, Germany). Phosphate buffered saline (PBS), pH 7.4, was prepared using of 40 mM NaOH, 40 mM NaH_2PO_4 and 150 mM NaCl. All solutions were freshly prepared before use.

2.2. Electrode preparation

Bare electrodes of 4 cm in length were freshly prepared by cutting 125 μm diameter Teflon coated Pt–Ir (90/10%) wire (Advent Research Material, U.K). Henceforth Pt–Ir is represented as Pt, as discussed previously by Kirwan et al., 2007; O'Neill et al., 2008). 1 mm of the Teflon coating was removed and the wire was soldered into a gold contact. The other end of the Pt wire was either cut transversely to produce a Pt disk (Pt_D), or ~2 mm of the Teflon was removed and cut to 1.0 mm, using a graduated eyeglass, to produce a Pt cylinder (Pt_C), as described previously by McMahon et al., 2005; McMahon and O'Neill, 2005.

2.3. Biosensor fabrication

Bare Pt electrodes were calibrated with H_2O_2 and AA before and after final modification. The PPD layer was produced by cyclic voltammetry at potential ranging from 0 to 1.0 V vs. Ag/AgCl and scan rate 100 mV s^{-1} for 15 cycles. The electro polymerization was carried out using BAS Epsilon, Bioanalytical System, USA. The resulting PPD-modified Pt electrodes were rinsed with PBS solution to remove the excess monomer. In some designs, Nafion (1% solution in alcohol) was deposited on the electrode surface by dip coating five times for 5 s periods. The deposited Nafion was alternately air dried between the dips for 5 min. The electrodes were conditioned in 25% aqueous glutaraldehyde (GA) for 5 min. Later, 600 U mL^{-1} DAAO (5950 U g^{-1} protein from Porcine Kidney, Biozyme Laboratories, UK) was chemisorbed onto the surface using GA by the dip and dip–spin coating procedure on the Pt_D and Pt_C wires, respectively. The biosensors were kept in the refrigerator at 4 °C to dry before use.

2.4. Calibrations

Amperometric calibrations (at +700 mV vs. Ag/AgCl) up to 100 μM H_2O_2 and up to 1000 μM AA were performed on all bare and modified Pt electrodes in quiescent N_2-saturated PBS. Linear regression was carried out to determine the calibration slopes (Prism 4.01, GraphPad Software Inc., San Diego, CA). Linear and nonlinear regression analysis was carried out on the steady state amperometric serine calibration data (at +700 mV) to determine the apparent Michaelis–Menten parameters, J_{max} and K_M, as well as the linear region slope, LRS, for D-serine and other prevalent D-amino acids in brain ECF. Calibrations were performed in a closed system in a standard three-electrode cell containing 20 mL N_2-saturated PBS at 25 ± 5 °C using 4-channel QuadStat (eDAQ, Australia). The current response was monitored using Chart software (eDAQ, Australia). Plots of averaged current density (J) vs. concentrations of D-amino acids, AA and H_2O_2 were then obtained.

2.5. In vivo experiments

Male Sprague Dawley rats weighing 250–325 g were procured from the Animal Care Facility, Universiti Sains Malaysia (USM), Pulau Pinang, Malaysia. The rats were anaesthetized with chlorolase/urethene (ethyl carbamate, 1.5 g/kg, i.p.) at the beginning of experiment. The rats were tracheotomised and breathed spontaneously. A femoral vein was cannulated for continuous intravenous infusion of 150 mmol NaCl initiated at 3 mL h^{-1} and the anesthetic at 1 mL h^{-1} (urethane/chlorolase, 180 and 12 mg, respectively, i.v.). A femoral artery was also cannulated for monitoring blood pressure and heart rate (Biopac System Instrument Inc., USA). The rat was then positioned onto a stereotaxic frame (Narishinge, Japan). The frontal skull was exposed for electrode implantation. The Pt_D/PPD/Naf/GA/DAAO and enzyme-devoid (blank) microbiosensors were implanted in the striatum. All coordinates were determined from bregma according to the atlas of Paxinos and Watson (1986). The measurements were made at +700 mV vs. Ag/AgCl using QuadStat. Animal handling and all procedures on animals were carried out in accordance with the guidelines of Animal Ethics Committee, USM, Pulau Pinang, Malaysia.

2.6. Data analysis

Current densities for substrate response, J_S (μA cm^{-2}), were used to compare biosensors current response of different biosensor geometries (Pt disk and Pt cylinder) in this work. Nonlinear regression analysis using Michaelis–Menten equation (Eq. (4)) of current density vs. substrate concentration [SER] plot provides the enzyme kinetics parameters: J_{max} and K_M, where J_{max} is the maximum J value at enzyme-substrate saturation. The apparent Michaelis constant, K_M, is the concentration of substrate that gives half of the J_{max} response. Regression coefficient, R^2, was obtained for the linear region slope (LRS) which generally valid up to half the Michaelis constant (K_M) value (O'Neill et al., 2008).

$$J_s = \frac{J_{max}}{1 + K_M/[SER]} \quad (4)$$

Apparent H_2O_2 permeability was defined by Eq. (5) to quantify and compare the ability of H_2O_2 species to permeate through the polymer-enzyme composite (PEC) film, while blocking AA access to the Pt,

$$P(HP)\% = \frac{\text{slope(HP) at Pt/PEC}}{\text{slope(HP) at bare Pt}} \times 100\% \quad (5)$$

where the slopes for H_2O_2 (HP) were obtained from linear regression analysis of the respective calibration plots for H_2O_2 at the same Pt electrodes, before and after the polymer-enzyme modification.

Polymer selectivity (S_{AA}%) has been usefully defined by Eq. (6) (Kirwan et al., 2007) or its equivalent (O'Neill et al., 2008), and represents the percentage interference by AA in H_2O_2 detection; thus the optimum value of S_{AA}% defined in this way is zero for biosensor applications. The use of equimolar concentrations in this definition allows S % to be interpreted as a permselectivity parameter for two analytes with the same z-value (electrons transferred per molecule), as is the case for AA and H_2O_2 (z = 2). AA concentration in tissue ECFs ranges from 50 μM in blood to 500 μM in brain

Table 1
Michaelis–Menten parameters (J_{max} and K_M) and linear region slopes (LRS) for biosensors of different enzyme immobilization designs.

Design	Electrode fabrication	n	J_{max} ($\mu A\,cm^{-2}$)	K_M (mM)	LRS ($\mu A\,cm^{-2}\,mM^{-1}$)
E1	Pt_D/GA/DAAO	4	117 ± 2	1.7 ± 0.6	45 ± 2
E2	Pt_D/PPD/GA/DAAO	4	73 ± 1	0.74 ± 0.15	54 ± 1
E3	Pt_D/Naf/GA/DAAO	4	103 ± 2	1.0 ± 0.2	49 ± 2
E4	Pt_D/PPD/Naf/GA/DAAO	4	91 ± 2	1.3 ± 0.1	63 ± 2
E5	Pt_D/Naf/PPD/GA/DAAO	4	78 ± 0.5	2.3 ± 0.1	34 ± 0.5
E6	Pt_C/GA/$DAAO_{(dip)}$/PPD	4	0.6 ± 3	6 ± 1	0.1 ± 1
E7	Pt_C/GA/$DAAO_{(dip-spin)}$/PPD	4	57 ± 8	1.5 ± 0.2	40 ± 8
E8	Pt_C/PPD/Naf/GA/$DAAO_{(dip-spin)}$	4	82 ± 5	1.8 ± 0.1	48 ± 4
E9	Pt_D/PEI/GA/DAAO/PPD	9	48 ± 10	1.6 ± 3	38 ± 8

(Miele and Fillenz, 1996), and can increase to millimolar levels during behavioral activation (Fillenz and O'Neill, 1986; O'Neill et al., 1983).

$$S_{AA}\% = \frac{I_{AA}(1\,mM)\,at\,Pt/PEC}{I_{HP}(1\,mM)\,at\,Pt/PEC} \times 100\% \quad (6)$$

When a biosensor incorporates a component that significantly affects the sensitivity of the surface to H_2O_2, e.g., Nafion, then variations in J_{max} across sensor populations may be due to changes in either enzyme activity or H_2O_2 sensitivity. The activity of surface enzyme itself depends on two factors: the density of active enzyme molecules on the surface (active enzyme loading, [E]) and the value of the catalytic rate constant, k_{cat}. Thus, enzyme activity is k_{cat}[E], and these two terms are rarely separable. A useful approximation to the effective activity of surface enzyme is the parameter $[E]_{act}$, defined in Eq. (7), where slope (HP) is the calibration slope for H_2O_2 at the biosensor PEC surface. Variations in $[E]_{act}$ determined under the same conditions will reflect changes in k_2[E], which in turn often arise from changes in [E] (McMahon et al., 2006).

$$[E]_{act} = \frac{J_{max}}{slope\,(HP)\,at\,Pt/PEC} \quad (7)$$

$$BE\% = \frac{LRS \times 100\%}{slope(HP)\,at\,Pt/PEC} \quad (8)$$

An analogous, and possibly more useful, parameter which also normalizes the biosensor response with respect to H_2O_2 sensitivity, is the biosensor efficiency (BE%) (see Eq. (8)) where LRS is the linear region slope for enzyme-substrate. In theory, the absolute maximum value of BE% should be 100% if the surface is saturated with enzyme, all the H_2O_2 produced by the enzyme were electro-oxidized on the surface, and the diffusion coefficients of enzyme-substrate (D_S) and H_2O_2 were equal. Since D_S will always be less than that for H_2O_2 ($\sim 1.0 \times 10^{-5}\,cm^2\,s^{-1}$) and some H_2O_2 is lost to the bulk even in quiescent solution (Lowry et al., 1994) then $(BE\%)_{max} < 100\%$. An empirical maximum appears to be close to 60% (McMahon et al., 2006), which is consistent with these factors.

Data were expressed as the mean ± standard error of mean (S.E.M.). Student's t-test was used to compare statistical differences between two data groups, with significance defined at $p < 0.05$. The value of n is the number of electrodes.

3. Results and discussion

3.1. Biosensor performances

Sensitivities of H_2O_2 and AA on the bare Pt_D electrodes were 177 ± 3 and 136 ± 2 $nA\,cm^{-2}\,\mu M^{-1}$ ($n = 7$), respectively, a ratio which is in line with that of their diffusion coefficients (Mikkelsen and Lennox, 1991; Ormonde and O'Neill, 1990) and indicative of hemispherical diffusion-controlled currents on the timescale of these constant potential amperometric measurements (Kirwan et al., 2007). The main concern in developing *in vivo* biosensors for neuroanalysis is not only to exclude interferences in brain ECF by using, say, a permselective polymeric membrane, but also to achieve the required permeability for transient H_2O_2 molecules generated by enzyme–substrate interaction. As observed previously (Dai et al., 2006; Killoran and O'Neill, 2008; Losito et al., 2003), the first cyclic voltammogram of the deposition of PPD indicated an irreversible electrode process of the polymerization (data not shown). After the 15 cycles used here, no further polymerization occurred due to the self sealing nature of PPD film. The PPD-modified electrodes that exhibited high H_2O_2 permeability, P(HP)% > 70% (see Eq. (5)) and low S_{AA} values < 0.5% (see Eq. (6)) were selected for further investigation.

DAAO immobilized via chemisorption with GA on the electrode led to a strong enzyme-support interaction (Lopez-Gallego et al., 2005) on the electrode surface. GA holds the enzyme via a three dimensional network, hence, keeping the enzyme biochemical properties intact and, consequently, provides an increment of J_{max} value (117 ± 2 $\mu A\,cm^{-2}$, $n = 4$, E1) as compared to the one without GA attachment (J_{max} = 1.3 ± 0.4 $\mu A\,cm^{-2}$, $n = 4$). The current density, J, of D-serine biosensors depends on the amount of active enzyme available on the electrode surface. The Michaelis–Menten parameters and LRS were determined using nonlinear and linear regression analyses for different enzyme immobilization designs as described elsewhere (O'Neill et al., 2008). Fig. 1 is the typical plot for parameters listed in Table 1 for the Pt_D/PPD/Naf/GA/DAAO (E4) design.

Design E4 (see Table 1) gave the best LRS value on account of its high J_{max} (good enzyme loading) and moderate value of K_M (enzyme–substrate affinity): LRS = J_{max}/K_M (O'Neill et al., 2008). As the LRS is the most important parameter from an analytical perspective (sensitivity in the linear response region), the majority of the experiments described below refer to this design: Pt_D/PPD/Naf/GA/DAAO.

The use of lower activity enzyme from other suppliers produced significantly less sensitive E4-type biosensors (data not shown).

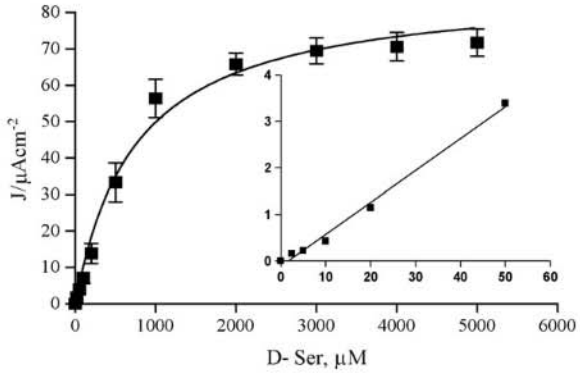

Fig. 1. The Michaelis–Menten nonlinear regression for the determination of J_{max} and K_M with corrected baseline (PBS subtracted) for Pt_D/PPD/Naf/GA/DAAO. Inset: Linear region of 0, 2.5, 5, 10, 20 and 50 μM D-serine showing a sensitivity of 61 ± 7 $\mu A\,cm^{-2}\,mM^{-1}$ ($n = 4$) and $R^2 = 0.999$.

Table 2
Comparison of performances among selected fabricated biosensors.

Parameters	Pt_D/PPD/GA/DAAO (E2, $n=4$)	Pt_D/Naf/ GA/DAAO (E3, $n=4$)	Pt_D/PPD/Naf/GA/DAAO (E4, $n=4$)
H_2O_2 slope (nA cm^{-2} μM^{-1})	125 ± 5	293 ± 6	177 ± 9
P(HP)%	71 ± 5	170 ± 6	100 ± 7
S_{AA}%	0.55 ± 0.5	0.54 ± 0.1	0.05 ± 0.1
$[E]_{act}$	60 ± 5	46 ± 3	91 ± 1
BE%	46 ± 2	33 ± 4	84 ± 1

Linear sensitivity obtained from 0 μM to 50 μM D-serine is 61 ± 7 μA cm^{-2} mM^{-1}, R^2 = 0.999 (n = 4). The limit of detection determined by three times the standard deviation of the baseline is 20 ± 1 nM (n = 8).

The pH dependence of the DAAO response to D-ser for the E4 design is shown in Fig. 2. The current density responses of Pt_D/PPD/Naf/GA/DAAO over the pH range from 6.4 to 10 were examined by changing the pH of the PBS. DAAO exhibits high activity at pH 8 and 9. However, at pH lower than 7 and higher than 10 the activity deteriorates markedly, which may be due to the formation of D-serine ions (pI_{SER} = 5.7 and pKa_2 = 9.2 (McMurray, 2004)) and the resultant modification of the tertiary structure of the protein (pI_{DAAO} = 7.0, 7.2 (Tishkov and Khoronenkova, 2005)).

Pt_D electrodes are particularly suitable for small regions of the brain and for studying layers of cells within regions, such as cerebral cortex. However, there are needs to study the relatively larger brain regions such as the dorsal striatum. Thus, 1 mm long cylinder Pt (Pt_C) wire biosensors (E6, E7 and E8) were also fabricated for comparison. The J_{max} value (0.6 ± 3 μA cm^{-2}, n = 4) of Pt_C/GA/DAAO/PPD (E6) which was fabricated following the Pt_D protocol, showed low accumulation of enzyme molecules on E6 electrodes due to enzyme drainage from the cylindrical side surface during the dip coating application of enzyme solution (McMahon and O'Neill, 2005). But this was overcome by the maximisation of the adhesion of enzyme molecules on the cylindrical side surface using a dip–spin protocol (E7 and E8). Remarkably, the J_{max} of 82 ± 5 μA cm^{-2} (n = 4) on E8 represents significant increment as compared to the E6 design. However, the J_{max} of this design was 50% less than the Pt_D designs and they also exhibited smaller LRS (48 ± 4 μA cm^{-2} mM^{-1}, n = 4) value compared to E4 design. From these results, it is clear that enzymatic sensitivities toward D-serine, reflected in the J_{max} and K_M values are dependent on the immobilization protocols and electrode geometry (Table 1). The effects of Pt geometry on parameters such as enzyme loading (McMahon et al., 2005; McMahon et al., 2007) and polymer permselectivity have been discussed previously by McMahon et al., 2004.

Polyethyleneimine (PEI in design E9) and Nafion (in designs E3 and E5) were applied as a first layer by dipping (~0.5 s) three and five times respectively. They were alternately air dried between the dips. From Table 1 it appears that the inclusions of the polycation PEI offers no significant effect on the enzymatic behaviour due to the similar sensitivity towards D-serine shown by configuration E9 and many other designs. It is worth noting that PEI has been used in biosensor designs to reduce electrostatic repulsion between substrate and glutamate oxidase (Lopez-Gallego et al., 2005; McMahon et al., 2007). But, since D-serine is neutral in pH 7.4 media, the lack of impact by PEI on the biosensor response is not too surprising.

Variation in J_{max} values determined under similar conditions, reflect differences in the activity of enzyme on the surface, provided that the sensitivity of the biosensor to H_2O_2 does not vary much (O'Neill et al., 2008). However, because some promising designs devised here did show differences in H_2O_2 sensitivity (see Table 2), two key parameters were normalized with respect to H_2O_2 sensitivity: active enzyme loading, [E_{act}] (Eq. (7)) and substrate sensitivity, BE% (Eq. (8)). Table 2 shows the relative performance of selected sensors. Good sensitivity towards H_2O_2 and ability to reject AA interference are two main parameters displayed. The selectivity coefficient vs. AA (S_{AA}%) (Eq. (6)) (O'Neill et al., 2008) is a good parameter in (i) comparing the H_2O_2 permselectivity of the biosensors and (ii) monitoring the effects of polymer layer in blocking AA interference on the electrode surface. The combination of PPD and Nafion (design E4) not only maintained H_2O_2 sensitivity but also enhanced AA blocking, providing a 10-fold improvement in S_{AA}% compared to the single layer of either PPD (design E2) or Nafion (design E3) alone. The excellent (low) value of S_{AA}% for the micro-disk design (E4) is somewhat surprising in view of the significant edge effects associated with this PPD-modified sensor size and geometry described recently by Rothwell et al. (2009). However, the incorporation of a cast Nafion layer in the E4 design, which coats and seals the Pt–Teflon edge (Brown et al., 2009), appears to neutralize the edge effect and improve permselectivity.

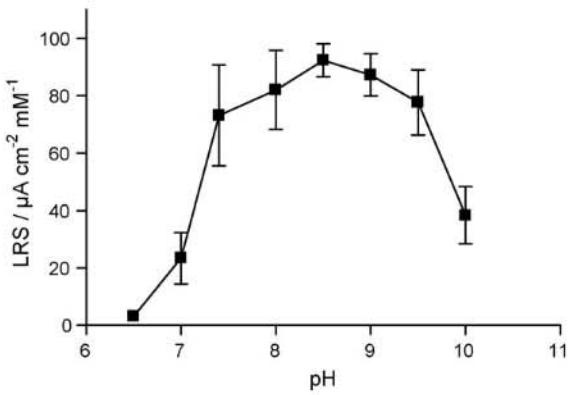

Fig. 2. Sensitivities (linear region slope) of Pt_D//PPD/Naf/GA/DAAO to D-serine at different pH.

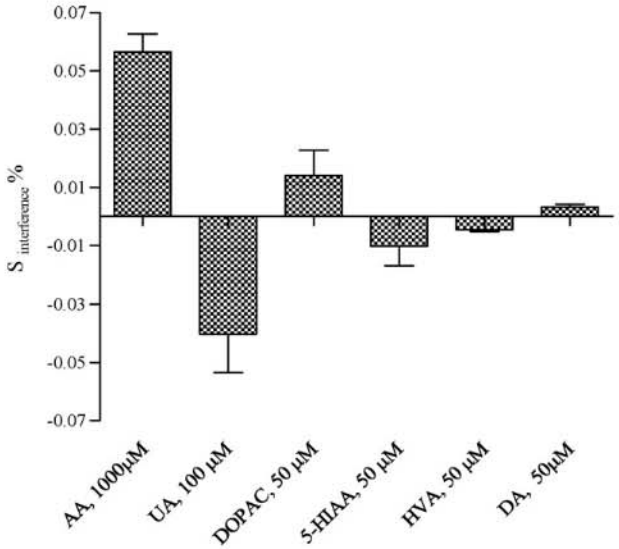

Fig. 3. Selectivity (%) (see Eq. (6) for AA, S_{AA}%) of interfering molecules present in ECF for Pt_D/PPD/Naf/GA/DAAO (n = 4).

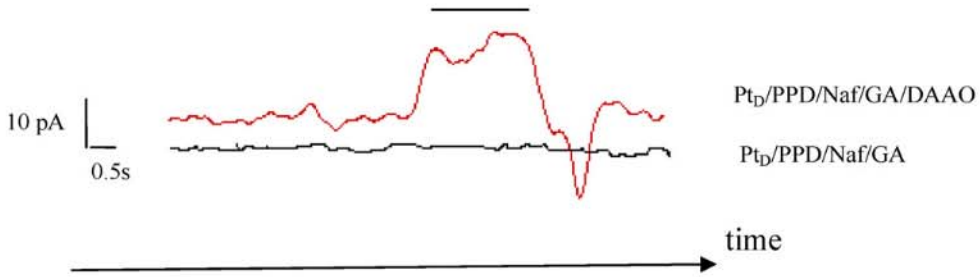

Fig. 4. The *in vivo* detection of D-serine in rat's striatum. Peak indicates 5 μL of 100 mM D-serine microinjected beside an implanted biosensor (E4) and corresponding "blank" sensor.

The $[E]_{act}$% and BE% values were used to investigate whether the PEC film modifications affected the biocatalytic functionality of the enzyme, DAAO. Biosensors of designs E2, E3 and E4 in Table 2 were characterized further since they showed good sensitivities towards H_2O_2 and D-serine. The inclusion of Nafion in the PPD film offered no significant effect on the enzymatic behaviour as shown from LRS values of E2 as compared to E3 ($p = 0.69$) and E4 ($p = 0.56$). The incorporation of Nafion after PPD did, however, decrease (improve) the S_{AA}% exhibited by E4. The increase in H_2O_2 sensitivity on E3 might be due to higher permeability of H_2O_2 from the leakage of H_2O_2 (Deng et al., 2007) decreased its $[E]_{act}$% and BE% values. The E4 fabrication not only exhibited highest $[E]_{act}$ and BE% but also the lowest S_{AA}% value. Hence, it is useful candidate for *in vivo* characterization.

The response time (0.7 ± 0.1 s, $n = 8$) of the sensor is faster because of thinner *ortho*-PPD used in this work compared to the *meta*-PPD deposition layer used (Killoran and O'Neill, 2008; Pernot et al., 2008). The high transport rates observed compared to cylindrical designs (Pernot et al., 2008) might be due to the efficient diffusion transport to micro-disk surface. Diffusion to cylindrical surface occurs in two dimensions and is less efficient than hemispherical diffusion to a micro-disk surface (Dayton et al., 1983). The lifetime (t_{L50}) in terms of sensitivity of fresh biosensors developed and kept in 4 °C was 6 months. The Pt$_D$/PPD/Naf/GA/DAAO (E4) is being used continuously within 3 days. No significant different in sensitivity (60 ± 1 μA cm^{-2} mM^{-1}, $n = 4$) was observed in day 2. However, sensitivity is decreased (55 ± 3 μA cm^{-2} mM^{-1}, $n = 4$) in day 3.

3.2. Interference studies

The developed biosensor (E4: Pt$_D$/PPD/Naf/GA/DAAO) also exhibited excellent chiral selectivity. It did not give any measurable linear response towards L-serine, L-alanine, L-cysteine and L-tyrosine in the concentration range of up to 5 mM. Apart from glycine, which is not a substrate for DAAO at physiological pH (Mothet et al., 2000), D-serine, D-aspartate and D-alanine are other D-amino acids prevalent in CNS. Current densities recordings with fixed potential amperometry following a series of spikes of these prevalent substrates were carried out to determine the level of enzyme–substrate specificity *in vitro*. No response was observed towards D-aspartate up to 0.1 mM. Substrate sensitivity for D-alanine was twice that for D-serine with LRS = 119 ± 5 μA cm^{-2} mM^{-1} ($n = 5$), as observed previously (Gabler et al., 2000). However, D-serine levels in brain ECF are about two orders of magnitude higher than those of D-alanine (Morikawa et al., 2001; Wolosker et al., 2002). Other neurochemicals like dopamine (50 μM), uric acid (100 μM), DOPAC (50 μM), 5-hydroxyindole acetic acid (50 μM) and homovanillic acid (20 μM) which are oxidisable at +700 mV (Brose et al., 1987) have also been tested for interference signatures on this design (see Fig. 3). Even at concentrations well in excess of baseline ECF levels, there were only marginal responses observed ($S_X\% < 0.06\%$, where x is the interference species).

3.3. Detection of D-serine in vivo

Given the success of the *in vitro* characterization described above for design E4 (Pt$_D$/PPD/Naf/GA/DAAO), this and other configurations were implanted in rat brain striatum, at coordinates (skull levelled between lambda and bregma): A/P +1 from bregma, M/L +1.3 and D/V -4 (from dura). Readings were taken in six rats acutely for each design. Mean baseline currents taken from 0 to 30 min at 40 Hz data sampling rate for (i) bare Pt$_D$, (ii) Pt$_D$/PPD and (iii) Pt$_D$/PPD/Naf/GA/DAAO were: 1.30 ± 0.08, -0.10 ± 0.04 and 0.35 ± 0.05 nA ($n = 6$), respectively. Fig. 4 shows that a steady state current (60 ± 0.01 pA, $n = 6$) was obtained from microinjection of 5 μL of 100 mM D-serine next to implanted E4 biosensors in order to validate that the DAAO remained immobilized and functional on the biosensor surface. Both the high concentration of infused D-serine needed and the current collapse following the infusion were due to diffusion and ECF tissue uptake of substrate. Such signals were not observed when a "blank" sensor (same design as E4, but omitting the enzyme) was implanted ($n = 6$; see Fig. 4).

4. Conclusions

This work has indicated that the sequence of polymers used, in this case Nafion and PPD, is a useful combination for getting the required response in the analysis of D-serine. The Pt$_D$/PPD/Naf/GA/DAAO design is capable of measuring D-serine without interference from most neurochemicals found in CNS, including its own enantiomer, ascorbate and other reducing agents. Work on the comparison between chiral selectivity and microdialysis analysis is underway and will be the subject of a future report. The proposed electrode is also useful for *in vivo* measurement of brain D-serine, and is presently undergoing extensive characterization *in vivo*.

Acknowledgement

This work was supported in part by funding from Science Foundation Ireland (SFI) and Eli Lilly (03/IN3/B376s). The financial supports from Ministry of Higher Education, Malaysia under Research University (RU) Grants: 1001/PKIMIA/811044 and 1001/PFARMASI/811053 are gratefully acknowledged. One of us (Z.M. Zain) is indebted to Universiti Teknologi MARA, Malaysia for granting study leave.

References

Bendikov, I., Nadri, C., Amar, S., Panizzutti, R., De Miranda, J., Wolosker, H., Agam, G., 2007. Schizophrenia Research 90 (1–3), 41–51.
Berna, M.J., Ackermann, B.L., 2007. Journal of Chromatography B 846 (1–2), 359–363.
Brose, N., O'Neill, R.D., Boutelle, M.G., Anderson, S.M.P., Fillenz, M., 1987. Journal of Neuroscience 7, 2917–2926.
Brown, F.O., Finnerty, N.J., Lowry, J.P. Analyst, doi:10.1039/b909005c.
Dai, Y.Q., Zhou, D.M., Shiu, K.K., 2006. Electrochimica Acta 52 (1), 297–303.

Dayton, M.A., Ewing, A.G., Wightman, R.M., 1983. Journal of Electroanalytical Chemistry 146, 189–200.
Deng, C., Li, M., Xie, Q., Liu, M., Yang, Q., Xiang, C., Yao, S., 2007. Sensors and Actuators B: Chemical 122 (1), 148–157.
Duff, A., O'Neill, R.D., 1994. Journal of Neurochemistry 62 (4), 1496–1502.
Durkin, T.A., Anderson, G.M., Cohen, D.J., 1988. Journal of Chromatography B: Biomedical Sciences and Applications 428, 9–15.
Fillenz, M., O'Neill, R.D., 1986. Journal of Physiology (London) 374, 91–100.
Fumero, B., Guadalupe, T., Valladares, F., Mora, F., O'Neill, R.D., Luis, J., Gonzalez, M., 1994. Journal of Neurochemistry 63 (4), 1407–1415.
Gabler, M., Hensel, M., Fischer, L., 2000. Enzyme and Microbial Technology 27 (8), 605–611.
Grant, S.L., Shulman, Y., Tibbo, P., Hampson, D.R., Baker, G.B., 2006. Journal of Chromatography B 844 (2), 278–282.
Hashimoto, A., Nishikawa, T., Oka, T., Takahashi, K., Hayashi, T., 1992. Journal of Chromatography: Biomedical Applications 582 (1–2), 41–48.
Hashimoto, A., Oka, T., Nishikawa, T., 1995. Neuroscience 66 (3), 635–643.
Katsuki, H., Nonaka, M., Shirakawa, H., Kume, T., Akaike, A., 2004. Journal of Pharmacology And Experimental Therapeutics 311 (2), 836–844.
Killoran, S.J., O'Neill, R.D., 2008. Electrochimica Acta 53 (24), 7303–7312.
Kirwan, S.M., Rocchitta, G., McMahon, C.P., Craig, J.D., Killoran, S.J., O'Brien, K.B., Serra, P.A., Lowry, J.P., O'Neill, R.D., 2007. Sensors 7, 420–437.
Lopez-Gallego, F., Betancor, L., Mateo, C., Hidalgo, A., Alonso-Morales, N., Dellamora-Ortiz, G., Guisan, J.M., Fernandez-Lafuente, R., 2005. Journal of Biotechnology 119 (1), 70–75.
Losito, I., Palmisano, F., Zambonin, P.G., 2003. Analytical Chemistry 75, 4988–4995.
Lowry, J.P., McAteer, K., El Atrash, S.S., Duff, A., O'Neill, R.D., 1994. Analytical Chemistry 66, 1754–1761.
Martineau, M., Baux, G., Mothet, J.P., 2006. Journal of Physiology-Paris 99 (2–3), 103–110.
Matsui, T.A., Sekiguchi, M., Hashimoto, A., Tomita, U., Nishikawa, T., Wada, K., 1995. Journal of Neurochemistry 65 (1), 454–458.
McMahon, C.P., Killoran, S.J., O'Neill, R.D., 2005. Journal of Electroanalytical Chemistry 580 (2), 193–202.
McMahon, C.P., O'Neill, R.D., 2005. Analytical Chemistry 77, 1196–1199.
McMahon, C.P., Rocchita, G., Serra, P.A., Kirwan, S.M., Lowry, J.P., O'Neill, R.D., 2006. Analyst 131, 68–72.
McMahon, C.P., Rocchitta, G., Kirwan, S.M., Killoran, S.J., Serra, P.A., Lowry, J.P., O'Neill, R.D., 2007. Biosensors and Bioelectronics 22 (7), 1466–1473.
McMahon, C.P., Killoran, S.J., Kirwan, S.M., O'Neill, R.D., 2004. Journal of Chemical Society Chemistry Communication, 2128–2130.
McMurray, J., 2004. Organic Chemistry, 6 ed. Thomson Learning, Inc, USA.
Miele, M., Fillenz, M., 1996. Journal of Neuroscience Methods 70 (1), 15–19.
Mikkelsen, S.R., Lennox, R.B., 1991. Analytical Biochemistry 195 (2), 358–363.
Mitala, C.M., Wang, Y., Borland, L.M., Jung, M., Shand, S., Watkins, S., Weber, S.G., Michael, A.C., 2008. Journal of Neuroscience Methods 174 (2), 177–185.
Morikawa, A., Hamase, K., Inoue, T., Konno, R., Niwa, A., Zaitsu, K., 2001. Journal of Chromatography B: Biomedical Sciences and Applications 757 (1), 119–125.
Mothet, J.P., Parent, A.T., Wolosker, H., Brady Jr., R.O., Linden, D.J., Ferris, C.D., Rogawski, M.A., Snyder, S.H., 2000. Proceedings of the National Academy of Sciences 97 (9), 4926–4931.
Mothet, J.P., 2001. Pathologie Biologie 49 (8), 655–659.
Nagata, Y., Borghi, M., Fisher, G.H., D'Aniello, A., 1995. Brain Research Bulletin 38 (2), 181–183.
O'Brien, K.B., 2005. Monitoring D-serine dynamics in the central nervous system by capillary electrophoresis. University of Minnesota.
O'Neill, R.D., Fillenz, M., Albery, W.J., 1983. Journal of Neuroscience Methods 8, 263–273.
O'Neill, R.D., Rocchitta, G., McMahon, C.P., Serra, P.A., Lowry, J.P., 2008. TrAC Trends in Analytical Chemistry 27 (1), 78–88.
Ormonde, D.E., O'Neill, R.D., 1990. Journal of Electroanalytical Chemistry 279 (1–2), 109–121.
Paxinos, G, Watson, C., 1986. The Rat Brain in Stereotaxic Coordinates, 2nd ed. Academic press, New York.
Pernot, P., Mothet, J.P., Schuvailo, O., Soldatkin, A., Pollegioni, L., Pilone, M., Adeline, M.T., Cespuglio, R., Marinesco, S., 2008. Analytical Chemistry 80, 1589–1597.
Pilone, M.S., 2000. Cellular and Molecular Life Sciences (CMLS) 57 (12), 1732–1747.
Quan, Z., Song, Y., Feng, Y., LeBlanc, M.H., Liu, Y.M., 2005. Analytica Chimica Acta 528 (1), 101–106.
Rothwell, S.A., Kinsella, M.E., Zain, Z.M., Serra, P.A., Rocchitta, G., Lowry, J.P., O'Neill, R.D., 2009. Analytical Chemistry 81, 3911–3918.
Tishkov, V.I., Khoronenkova, S.V., 2005. Biochemistry (Moscow) 70, 40–54.
Wolosker, H., Panizzutti, R., Miranda, J.D., 2002. Neurochemistry International 41 (5), 327–332.
Xie, X., Dumas, T., Tang, L., Brennan, T., Reeder, T., Thomas, W., Klein, R.D., Flores, J., O'Hara, B.F., Heller, H.C., Franken, P., 2005. Brain Research 1052 (2), 212–221.